Sensors and Materials, Vol. 28, No. 11 (2016) 1203–1210
MYU Tokyo

S & M 1281

Investigation on Reduction Behaviors of SnO_2 and SnO_2-Supported CuO Sensor Materials by Temperature-Programmed Reduction Method Combined with Resistance Measurement

Hiroyuki Yamaura, Shinsuke Hirao, Syuhei Yamaguchi, and Hidenori Yahiro*

Department of Materials Science and Biotechnology, Graduate School of Science and Engineering, Ehime University, Matsuyama, Ehime 790-8577, Japan

(Received May 30, 2016; accepted August 15, 2016)

Keywords: TPR measurement, resistance measurement, semiconductor, tin oxide, copper oxide

Temperature-programmed reduction measurement combined with resistance measurement (TPR&R) was performed to investigate the reduction behavior of the samples containing the semiconductor materials, SnO_2 and CuO/SnO_2. The four reduction peaks were observed in the H_2-TPR profile of SnO_2, being assigned to the reductions of surface adsorbed oxygen species, surface lattice oxygen, amorphous SnO_2 and bulk SnO_2. On the other hand, the H_2-TPR profile of CuO/SnO_2 was more complicated than that of SnO_2. The TPR&R measurement enabled definite assignments of the six reduction peaks of CuO/SnO_2: the reductions of (I) Cu^{2+} to Cu^+ in highly dispersed copper oxide, (II) bulk CuO to Cu^0, (III) Cu^+ to Cu^0 in highly dispersed copper oxide, (IV) SnO_2 lattice oxygen interacting with highly dispersed copper oxide, (V) amorphous SnO_2, and (VI) bulk SnO_2.

1. Introduction

CuO-doped SnO_2 has been reported to be one of the potential materials for CO[1–3] sensors. We have demonstrated that CuO-doped SnO_2 exhibited a response to the small amount of CO involving H_2 flow and that its response was related with the oxidation states of Cu and Sn.[3] Therefore, the investigation of the reduction behavior of CuO-doped SnO_2 is significant for understanding the sensor mechanism.

It is well known that temperature-programmed reduction (TPR) measurement is one of the most powerful techniques for elucidating the reduction behavior of a material containing a noble metal, a transition metal oxide, or a lanthanide metal oxide. Numerous TPR studies on copper oxides have been reported, for example, CuO/CeO_2,[4] $CuO/Ti_xSn_{1-x}O_2$,[5] CuO/Al_2O_3,[6] $Cu\text{-}Fe/Al_2O_3$,[7] and $K\text{-}Cu/Al_2O_3$,[8] for clarifying the active copper site for CO oxidation,[4,5] water–gas shift reaction,[6,7] NO_x reduction,[8] among others. Arino *et al.*[9] reported that the TPR profile of SnO_2 exhibited four reduction peaks at 250, 310, 420, and >470 °C and that the loading of Pt or Pd promoted the reduction of SnO_2; that is, four reduction peaks shifted to a lower temperature by loading Pt or Pd on SnO_2. A similar result was reported by Pavelko *et al.*[10] The TPR profile of a metal oxide

*Corresponding author: e-mail: hyahiro@ehime-u.ac.jp

ISSN 0914-4935

supported on SnO_2 was more complicated than that of a metal oxide supported on a thermally stable material such as Al_2O_3 and SiO_2, because of the contribution of the reduction of SnO_2 itself; therefore, the appearance of TPR reduction peaks for SnO_2-supported materials remains ambiguous.

In the present study, TPR measurement combined with resistance measurement was carried out to better understand the reduction behavior of the samples containing the semiconductor materials, SnO_2 and CuO/SnO_2. In addition, X-ray diffraction (XRD) and diffuse-reflectance infrared Fourier transform-infrared (DRIFT-IR) measurements were performed to obtain additional evidence for supporting the assignments of the TPR peaks of SnO_2 and CuO/SnO_2.

2. Experimental Methods

SnO_2 was prepared by the ammonolysis of a solution of tin chloride (Kishida Chem., 99%) according to a previously reported method.[11] The resulting precipitate was washed repeatedly with deionized water and then calcined at 600 °C for 5 h to yield SnO_2. CuO was loaded on SnO_2 powder by a conventional impregnation method with an aqueous solution of $Cu(CH_3COO)_2 \cdot H_2O$ (Kanto Chem., 99%). The loaded sample was finally calcined at 600 °C for 5 h. The loading amount of CuO was 2–30 wt%. The sample is represented by $CuO(x)/SnO_2$, where x is the loading amount of CuO.

A schematic view of the experimental apparatus for TPR measurement combined with the resistance measurement is shown in Fig. 1. The redox behavior and the change in the sample resistance can be measured using this apparatus. This new combined method is named "TPR&R" hereafter. The element for measuring sample resistance was fabricated by the following method.[11] The sample powder was dispersed in deionized water, and the resulting paste was painted on an alumina tube (1.2 mmϕ) with a pair of Pt wire electrodes attached. The element with the sample was located in the middle of a quartz tube (9 mmϕ) and the sample resistance was determined by measuring the voltage of external resistance, as shown in Fig. 1.

For TPR measurement, the sample powder was pressed and sieved in the range of 212–500 μm. 0.2 g of the granular sample was placed near the element for measuring sample resistance (Fig. 1).

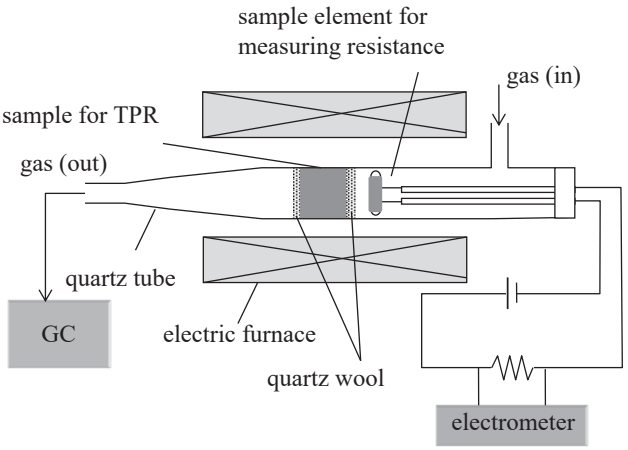

Fig. 1. Schematic view of experimental apparatus of TPR&R measurement.

The amount of H_2 consumed was monitored using a gas chromatograph (Shimadzu, GC-8AIT) with a thermal conductivity detector (TCD).

Prior to TPR&R measurement, the samples were pretreated at 500 °C for 3 h in air. TPR&R measurement was carried out by flowing 5 vol% H_2 + N_2 (50 $cm^3 \cdot min^{-1}$) in the temperature range of 50–450 °C at a heating rate of 2 $°C \cdot min^{-1}$.

DRIFT-IR spectra were recorded while flowing pure N_2 at room temperature or 50 vol% H_2 (N_2 balance) at 50, 300, and 350 °C with a Perkin Elmer Spectrum One spectrometer. Powder XRD analysis was performed to determine the crystalline phase of samples using a Rigaku RINT2200HF diffractometer with CuKα radiation.

3. Results

3.1 XRD profiles of CuO/SnO_2 and SnO_2 samples

The XRD profiles of $CuO(x)/SnO_2$ and SnO_2 samples are shown in Fig. 2. The strong peaks assigned to the tetragonal crystal phase of SnO_2 were observed at 33, 37, and 39°.[2] For $CuO(2)/SnO_2$ with a small loading amount of CuO, there were no detectable XRD peaks induced from CuO crystallites. As the loading amount of CuO increased, the crystal phase of CuO became apparent at 35, 38, and 49°, and these peaks of CuO were intensified. The XRD results suggest that CuO is highly dispersed on SnO_2 when the loading amount of CuO is smaller than 5 wt%, and the excess loading of copper (more than 5 wt%) forms bulk CuO, which can be reflected in the XRD pattern.[4] The crystalline sizes of SnO_2 and CuO in $CuO(x)/SnO_2$, which were estimated from SnO_2(101) and CuO(002) XRD peaks using the Scherrer's equation, are summarized in Table 1, being less dependent on the loading amount of CuO.

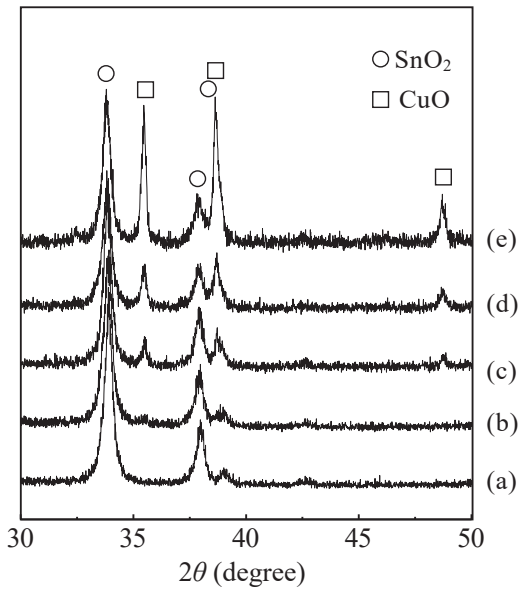

Fig. 2. XRD patterns of (a) SnO_2, (b) $CuO(2)/SnO_2$, (c) $CuO(5)/SnO_2$, (d) $CuO(8)/SnO_2$, and (e) $CuO(15)/SnO_2$. ○: SnO_2 and □: CuO.

3.2 DRIFT-IR spectra of SnO_2

The *in situ* DRIFT-IR spectra of SnO_2 exposed to 50 vol% H_2 + N_2 at 50, 300, and 350 °C for 2 h are shown in Fig. 3. The spectra shown in Fig. 3 represent the change in the spectra before and after the respective treatments, that is, the negative peak indicates the decrease in the amount of surface species accompanying desorption and/or decomposition. The DRIFT-IR spectra of SnO_2 exposed to 50 vol% H_2 + N_2 at 300 and 350 °C showed a strong negative peak in the region assigned to Sn–O–Sn stretching vibration (750–2000 cm^{-1}).[13] The result suggests that SnO_2 was reduced by 50 vol% H_2 + N_2 at the temperature above 300 °C.

3.3 TPR&R profiles of SnO_2 and CuO/SnO_2

The TPR&R profiles of SnO_2 and CuO(x)/SnO_2 samples (x = 2, 5, 8, 15, and 30) are shown in Fig. 4. The overlapping reduction peaks in the TPR profiles shown in Figs. 4(a)–4(f) were deconvoluted, as shown in Figs. 4(a′)–4(f′), respectively. SnO_2 provided four TPR peaks centered at 230 (peak α), 300 (peak β), 370 (peak γ), and >400 °C (peak ω) [Figs. 4(a) and 4(a′)]. A similar result was reported by Arino *et al.*[9] The reduction peaks α and β were accompanied by a decrease and an increase in resistance, respectively, whereas the reduction peaks γ and ω contributed less to the change in resistance.

Table 1
Amounts of H_2 consumption for the reduction peaks I, II, III, and IV in TPR profiles of CuO(x)/SnO_2 samples.

Sample	Mole of CuO loaded[a] (μmol)	Crystallite size[b] of SnO_2 (nm)	Crystallite size[b] of CuO (nm)	Amounts of H_2 consumption[c] (μmol)			
				Peak I	Peak II	Peak III	Peak IV
$CuO(2)/SnO_2$	57	21	—	29 (145)	—	32 (213)	41 (250)
$CuO(5)/SnO_2$	142	23	42	64 (137)	17 (183)	70 (212)	110 (240)
$CuO(8)/SnO_2$	228	19	36	53 (151)	110 (242)	57 (212)	104 (266)
$CuO(15)/SnO_2$	438	23	36	48 (146)	345 (237)	42 (216)	94 (254)
$CuO(30)/SnO_2$	848	19	31	41 (140)	769 (226)	42 (203)	51 (266)

[a]The weight of the material for TPR measurement was unified to be 0.2 g.
[b]The crystallite size was estimated using Scherrer's equation.
[c]The numerical values in parenthesis indicate the temperatures of peak top.

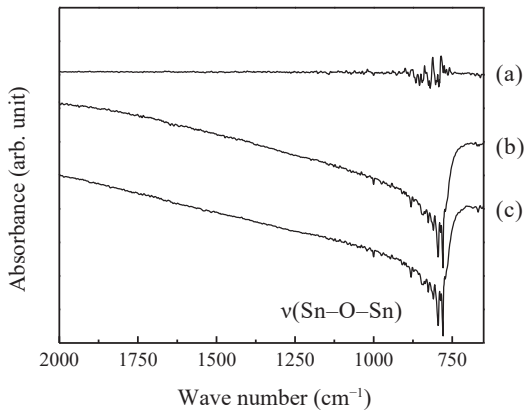

Fig. 3. DRIFT-IR spectra of SnO_2 after exposure to 50 vol% H_2/N_2 at (a) 50, (b) 300, and (c) 350 °C for 2h.

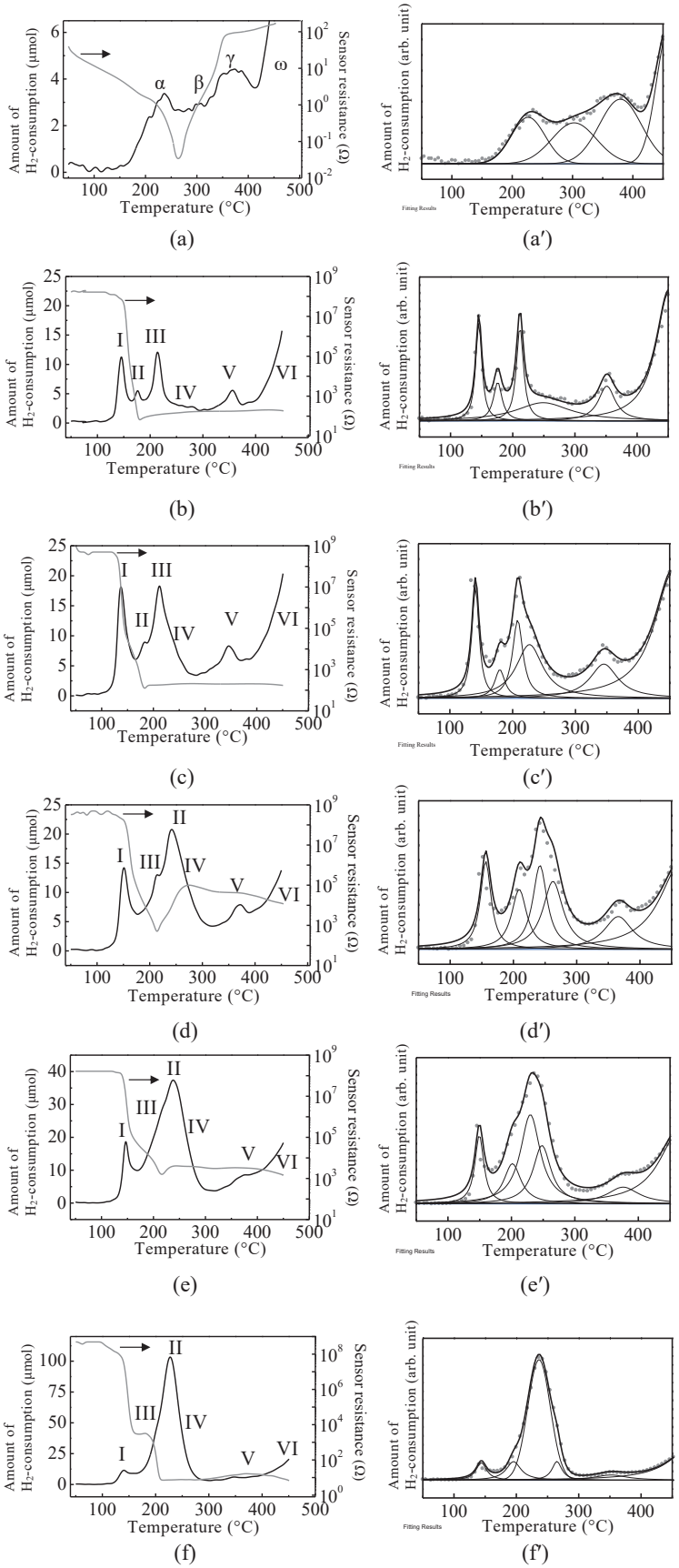

Fig. 4. TPR&R profiles of (a) SnO_2, (b) CuO(2)/SnO_2, (c) CuO(5)/SnO_2, (d) CuO(8)/SnO_2, (e) CuO(15)/SnO_2, and (f) CuO(30)/SnO_2, and the deconvolution curves of TPR profile for (a′) SnO_2, (b′) CuO(2)/SnO_2, (c′) CuO(5)/SnO_2, (d′) CuO(8)/SnO_2, (e′) CuO(15)/SnO_2, and (f′) CuO(30)/SnO_2.

Figure 4(b) shows the TPR&R profile of CuO(2)/SnO_2. The TPR profile of CuO(2)/SnO_2 was more complicated than that of SnO_2. The TPR profile of CuO(2)/SnO_2 consisted of six reduction peaks represented by peaks I–VI, as shown in Fig. 4(b). A similar TPR&R profile was obtained for CuO(5)/SnO_2 [Figs. 4(c) and 4(c′)]. The amounts of H_2 consumed for peaks I–IV are summarized in Table 1. The TPR profiles of CuO(8)/SnO_2, CuO(15)/SnO_2, and CuO(30)/SnO_2 with higher Cu loading [Figs. 4(d)–4(f) and 4(d′)–4(f′)] were slightly different from those of CuO(2)/SnO_2 and CuO(5)/SnO_2 with lower Cu loading; the position of peak II shifted to a higher temperature.

All samples of CuO(x)/SnO_2 showed much higher resistance than SnO_2 at low temperature (50–150 °C). With increasing temperature, the sample resistance markedly decreased to 180–220 °C, together with the appearance of peak I, and then slightly increased. In the intermediate temperature range (180–300 °C), the change in the sample resistance of CuO(x)/SnO_2 was dependent on the amount of CuO loaded on SnO_2. The high resistance augmentation was observed for CuO(8)/SnO_2. In the high temperature range (>300 °C), the sample resistance was less sensitive to temperature, although the reduction peaks V and VI were observed.

4. Discussion

4.1 Assignments of reduction peaks in TPR profile of SnO_2

TPR studies of SnO_2-based materials have been reported by several researchers.[9–12] Sasikala *et al.*[12] reported that a series of TPR peaks observed at low temperature were assigned to the reduction of the SnO_2 surface. Pavelko *et al.*[10] reported that the reduction peaks of SnO_2 below 450 °C were attributed to the reduction of not only the surface but also the subsurface of SnO_2. Thus, the assignment of the TPR reduction peak to SnO_2 is still controversial; therefore, we attempted to assign the TPR reduction peaks of SnO_2 by TPR&R measurement.

The α peak in Fig. 4(a), accompanied by a significant decrease in sample resistance, can be assigned to the reduction of anionic surface-adsorbed oxygen species such as O_2^- and O^- because of the following reason. When the anionic surface-adsorbed oxygen species that trapped electrons from SnO_2 are reacted with H_2 gas, the electrons from the anionic species are donated to SnO_2, resulting in the decrease in the sample resistance. A similar explanation concerning the TPR peak was reported by Marikutsa *et al.*[13]

In contrast to the α peak, the β peak observed at 300 °C was accompanied by an increase in sample resistance. DRIFT-IR spectra shown in Fig. 3 demonstrated that SnO_2 was partially reduced when the SnO_2 sample was exposed to 50 vol%H_2 + N_2 at 300 °C. Therefore, the β peak may be assigned to the reduction of the lattice oxygen of SnO_2, probably near the surface. The presumable interpretation of resistance augmentation is as follows. The lattice oxygen of SnO_2 was reduced to form SnO, which is a p-type semiconductor. The p-type SnO forms a p–n heterojunction with an unreduced n-type SnO_2 bulk, resulting in the increase in sample resistance. Although there is no direct evidence of SnO formation in this study, Kulshreshtha and Gadgil[14] reported the formation of SnO as an intermediate phase during the H_2 reduction of SnO_2.

During the appearance of the γ peak, no change in sample resistance was observed so that the assignment of the γ peak is difficult from TPR&R measurement. The assignment of the γ peak will be discussed in the following section.

The intensity of the ω peak was markedly increased at >400 °C. This suggests that the reduction of the lattice oxygen in SnO_2 progressively proceeded with increasing reduction temperature. This assumption was supported by the DRIFT-IR result that the negative peak derived from ν(Sn–O–Sn) became large with increasing reduction temperature (Fig. 3). Therefore, the ω peak can be assigned to the reduction of bulk SnO_2.

4.2 Assignments of reduction peaks in TPR profiles of SnO_2-supported CuO

As shown in Figs. 4(b)–4(f) and 4(b′)–4(f′), CuO(x)/SnO_2 samples exhibited six reduction peaks, peaks I–VI, regardless of the loading amount of CuO. As can be seen in Figs. 4(b)–4(f), it is clear that peak I of all the CuO(x)/SnO_2 samples was accompanied by the marked decrease in resistance. The initial high resistance of CuO(x)/SnO_2 samples (>10^9 Ω) may be derived from n-SnO_2/p-CuO heterojunctions between the supported p-type CuO grains and the n-type SnO_2 grains.[15] Upon exposure to H_2 gas in TPR&R measurement, the barrier height of n-SnO_2/p-CuO heterojunctions decreases markedly because of the partial reduction of p-CuO to CuO_{1-x}, probably leading to a marked decrease in resistance. Therefore, peak I can be assigned to the reduction of CuO.

The amounts of H_2 consumed for peaks I and III were increased with increasing loading amount of CuO, reaching a maximal value for CuO(5)/SnO_2, and then decreased with the further increase in the loading amount of CuO (Table 1). In addition, the amount of H_2 consumption for peak I was almost equal to that for peak III. Therefore, it is presumable that peaks I and III come from the reduction of identical CuO species. As can be seen in Fig. 2, the XRD pattern of CuO(2)/SnO_2 exhibited no visible diffraction peak because of the high dispersion of CuO, whereas peaks I and III were clearly observed in Fig. 4(b). As a result, peaks I and III were tentatively assigned to the reduction of Cu^{2+} to Cu^+ and Cu^+ to Cu^0, respectively, of highly dispersed CuO.

$$\text{Peak I: } 2CuO + H_2 \rightarrow Cu_2O + H_2O$$

$$\text{Peak III: } Cu_2O + H_2 \rightarrow 2Cu^0 + H_2O$$

As shown in Fig. 2, the increase in the loading amount of CuO from 8 to 30 wt% resulted in the increase in the intensity of the diffraction peaks of CuO. Table 1 shows that the amount of H_2 consumption for peak II was increased with increasing CuO loading from 8 to 30 wt%, and the total amounts of H_2 consumption for peaks I, II, and III corresponded to the amount of H_2 consumption required for the complete reduction of CuO to metallic Cu. Therefore, peak II can be assigned to the reduction of bulk CuO.

Interestingly, the behavior of peak IV was similar to those of peaks I and III, suggesting that peak IV was related to highly dispersed CuO. In addition, the sample resistance increased together with the appearance of peak IV. Since the total amount of H_2 consumption for peaks I, II, and III corresponded to that of the complete reduction of CuO to metallic copper, the origin of peak IV cannot be explained by the reduction of CuO species. Liu *et al.*[16] reported that the CuO fine particles in intimate contact with cerium oxide showed “strong interaction” and promoted the surface reduction of cerium oxide. Considering this report, peak IV is probably assigned to the reduction of the surface lattice oxygen of SnO_2 interacted with highly dispersed CuO. The increase in sample resistance may be derived from the p–n heterojunction of reduced SnO_2 with the p-type semiconductor with an unreduced SnO_2 bulk with the n-type semiconductor.

The temperatures giving peaks V and VI were almost the same as those giving peaks γ and ω in Fig. 4(a), respectively. This result implies that peaks V and VI are identical to peaks γ and ω, respectively. As mentioned in a previous section, peak ω (peak VI) can be assigned to the reduction of bulk SnO_2. The assignment of peak γ (peak V) could not be clarified in the present study; however, Park *et al.*[17] pointed out that the TPR peak of a SnO_2/Al_2O_3 catalyst below 450 °C was assigned to the reduction of amorphous SnO_2.

The present TPR&R measurement proved the reduction of SnO_2 with several overlapping peaks in the temperature range of 200–300 °C. In addition, the stepwise reduction of highly dispersed CuO (+2 → +1 → 0) was clarified and the resulting reduced copper species was found to play a role as a promoter of the reduction of SnO_2.

5. Conclusions

The resistance measurement was combined with TPR measurement (TPR&R) to assign the reduction peaks in the TPR profiles of SnO_2 and CuO(x)/SnO_2. Using TPR&R, the four reduction peaks in TPR profile of SnO_2 at 230, 300, 370, and >400 °C could be assigned to the reduction of oxygen species adsorbed on SnO_2, lattice oxygen of SnO_2 near the surface, amorphous SnO_2, and bulk SnO_2, respectively. In the TPR profile of CuO(x)/SnO_2, the experimentally observed six peaks, peaks I–VI, were found to be attributed to the reductions of (I) Cu^{2+} to Cu^+ in highly dispersed copper oxide, (II) bulk CuO to Cu^0, (III) Cu^+ to Cu^0 in highly dispersed copper oxide, (IV) SnO_2 lattice oxygen interacting with highly dispersed copper oxide, (V) amorphous SnO_2, and (VI) bulk SnO_2. Thus, TPR&R measurement is one of the powerful methods enabling the definite assignment of the reduction peaks of materials containing a semiconductor such as SnO_2 and CuO(x)/SnO_2.

References

1 S. Bai, W. Guo, J. Sun, J. Li, Y. Tian, A. Chen, R. Luo, and D. Li: Sens. Actuators, B **226** (2016) 96.
2 G. Zhang and M. Liu: Sens. Actuators, B **69** (2000) 144.
3 H. Yamaura, Y. Iwasaki, S. Hirao, and H. Yahiro: Sens. Actuators, B **153** (2011) 465.
4 M. F. Luo, Y. J. Zhong, X. X. Yuan, and X. M. Zheng: Appl. Catal., A **162** (1997) 121.
5 J. Huang, S. Wang, X. Guo, D. Wang, B. Zhu, and S. Wu: Catal. Commun. **9** (2008) 2131.
6 H. Yahiro, K. Sagata, T. Yamamoto, K. Saiki, M. Asamoto, and H. Yamaura: Catal. Lett. **124** (2008) 233.
7 K. Sagata, Y. Kawanishi, M. Asamoto, H. Yamaura, and H. Yahiro: Chem. Lett. **38** (2009) 172.
8 N. Nejar and M. J. Illan-Gomez: Appl. Catal., B **70** (2007) 261.
9 M. D. Arino, F. Pinna, and G. Strukul: Appl. Catal., B **53** (2004) 161.
10 R. G. Pavelko, A. A. Vasiliev, E. Llobet, X. Vilanova, N. Barrabés, F. Medina, and V. G. Sevastyanov: Sens. Actuators, B **137** (2009) 637.
11 H. Yamaura, M. Nakaoka, S. Hirao, A. Fujiwara, and H. Yahiro: Mater. Manuf. Process. **25** (2010) 350.
12 R. Sasikala, N. M. Gupta, and S. K. Kulshreshtha: Catal. Lett. **71** (2001) 69.
13 A. V. Marikutsa, M. N. Rumyantseva, L. V. Yashina, and A. M. Gaskov: J. Solid State Chem. **183** (2010) 2389.
14 S. K. Kulshreshtha and M. M. Gadgil: Appl. Catal., B **11** (1997) 291.
15 L. A. Patil and D. R. Patil: Sens. Actuators, B **120** (2006) 316.
16 W. Liu and M. F. Stephanopoulos: Chem. Eng. J. **64** (1996) 283.
17 P. W. Park, H. H. Kung, D. W. Kim, and M. C. Kung: J. Catal. **184** (1999) 440.